THE JOURNAL OF BIOLOGICAL CHEMISTRY
Vol. 279, No. 20, Issue of May 14, pp. 21193–21199, 2004

Printed in U.S.A.

Functional Significance of Conserved Histidines and Arginines in the 49-kDa Subunit of Mitochondrial Complex I*

Received for publication, December 3, 2003, and in revised form, February 11, 2004
Published, JBC Papers in Press, March 5, 2004, DOI 10.1074/jbc.M313180200

Ljuban Grgic, Klaus Zwicker, Noushin Kashani-Poor, Stefan Kerscher, and Ulrich Brandt‡

From the Institut für Biochemie I, Fachbereich Medizin, Universität Frankfurt, D-60590 Frankfurt am Main, Germany

We have studied the ubiquinone-reducing catalytic core of NADH:ubiquinone oxidoreductase (complex I) from *Yarrowia lipolytica* by a series of point mutations replacing conserved histidines and arginines in the 49-kDa subunit. Our results show that histidine 226 and arginine 141 probably do not ligate iron-sulfur cluster N2 but that exchanging these residues specifically influences the properties of this redox center. Histidines 91 and 95 were found to be essential for ubiquinone reductase activity of complex I. Mutations at the C-terminal arginine 466 affected ubiquinone affinity and inhibitor sensitivity but also destabilized complex I. These results provide further support for a high degree of structural conservation between the 49-kDa subunit of complex I and its ancestor, the large subunit of water-soluble [NiFe] hydrogenases. In several mutations of histidine 226, arginine 141, and arginine 466 the characteristic EPR signatures of iron-sulfur cluster N2 became undetectable, but specific, inhibitor-sensitive ubiquinone reductase activity was only moderately reduced. As we could not find spectroscopic indications for a modified cluster N2, we concluded that these complex I mutants were lacking most of this redox center but were still capable of catalyzing inhibitor-resistant ubiquinone reduction at near normal rates. We discuss that this at first surprising scenario may be explained by electron transfer theory; after removal of a single redox center in a chain, electron transfer rates are predicted to be still much faster than steady-state turnover of complex I. Our results question some of the central mechanistic functions that have been put forward for iron-sulfur cluster N2.

The respiratory chain of the inner membrane of mammalian mitochondria consists of four enzyme complexes and creates the transmembrane protonmotive force used by ATP synthase to generate ATP. Complex I (NADH:ubiquinone oxidoreductase) is the largest and least understood of these multisubunit complexes. It oxidizes NADH to NAD^+ and transfers electrons via FMN and up to eight iron-sulfur clusters to ubiquinone that is reduced to ubiquinol (1). Pumping of 4 H^+/2 electrons across the inner mitochondrial membrane is coupled to this process. Since cluster N2 has been shown to couple magnetically with semiquinone (2), it is likely to be the immediate reductant for ubiquinone at the end of the electron transfer cascade formed by the iron-sulfur clusters of complex I.

In recent years we have established the obligate aerobic yeast *Yarrowia lipolytica* as a model to study structure and function of complex I (3). Based on a site-directed mutagenesis study we have proposed that the ubiquinone-reducing catalytic core of complex I has evolved from the active center of [NiFe] hydrogenases and resides at the interface between the 49-kDa and the PSST subunits (4, 5). The 49-kDa subunit is homologous to the large and the PSST subunit to the small subunit of bacterial water-soluble [NiFe] hydrogenases (6, 7) for which x-ray structures have been solved (8, 9). Of the three iron-sulfur clusters bound to the small subunit of these hydrogenases only the proximal one is retained as cluster N2 in the PSST subunit of complex I (10, 11). However, in all PSST subunits sequenced so far, only three of the four cysteines are left that ligate the proximal cluster in the small subunit of hydrogenases. A fourth cysteine is found immediately adjacent to the first of these three conserved cysteines in all known PSST sequences; for steric reasons, it has been generally considered unlikely that the resulting putative Cys-Cys-X_n-Cys-X_n-Cys motif ligates iron-sulfur cluster N2. However, this option has been put forward recently by Flemming *et al.* (12). The earlier idea that an acidic residue may serve as the fourth ligand of cluster N2 (13) could be ruled out by mutating every single conserved aspartate and glutamate in the PSST subunit (5). As cluster N2 is predicted to reside immediately at the interface between the two subunits, we have suggested that the missing fourth ligand may be provided by the adjacent 49-kDa subunit (4).

To explore this possibility and to gain further insight into structure-function relationships within the ubiquinone-reducing catalytic core of complex I, we have analyzed mutations of highly conserved histidines and arginines in the 49-kDa subunit of complex I (Fig. 1). The residues chosen for mutagenesis were predicted to be in the vicinity (within about 15 Å) of iron-sulfur cluster N2 based on the previously demonstrated conservation of the [NiFe] hydrogenase structural fold (4).

MATERIALS AND METHODS

Substrates and Inhibitors—2-*n*-Decylubiquinone (DBQ),[1] deamino-NADH (dNADH), hexammine ruthenium(III) chloride (HAR), and rotenone were purchased from Sigma; hygromycin B was purchased from Invitrogen; and 2-decyl-4-quinazolinyl amine (DQA) was a generous gift from Aventis CropScience (Frankfurt am Main, Germany).

Strains—Y. lipolytica haploid strain Δnucm L1 (*nucm*::*URA3*, *Mat*A, *30Htg2*, *ndh2i*, *lys11–23*, *ura3–302*, *leu2–270*, *xpr2–322*) was made by mating strain NK2.1 (*nucm*::*URA3*, *Mat*A, *ndh2i*, *lys11–23*, *ura3–302*,

* This work was supported by the Deutsche Forschungsgemeinschaft, Sonderforschungsbereich 472, P2 and the Fonds der Chemischen Industrie. The costs of publication of this article were defrayed in part by the payment of page charges. This article must therefore be hereby marked "*advertisement*" in accordance with 18 U.S.C. Section 1734 solely to indicate this fact.

‡ To whom correspondence should be addressed: Universität Frankfurt, Fachbereich Medizin, Institut für Biochemie I, Theodor-Stern-Kai 7, Haus 25B, D-60590 Frankfurt am Main, Germany. Tel.: 49-69-6301-6926; Fax: 49-69-6301-6970; E-mail: brandt@zbc.kgu.de.

[1] The abbreviations used are: DBQ, 2-*n*-decylubiquinone; dNADH, deamino-NADH; HAR, hexammine ruthenium(III) chloride; DQA, 2-decyl-4-quinazolinyl amine; MOPS, 4-morpholinepropanesulfonic acid; mW, milliwatt; mT, millitesla.

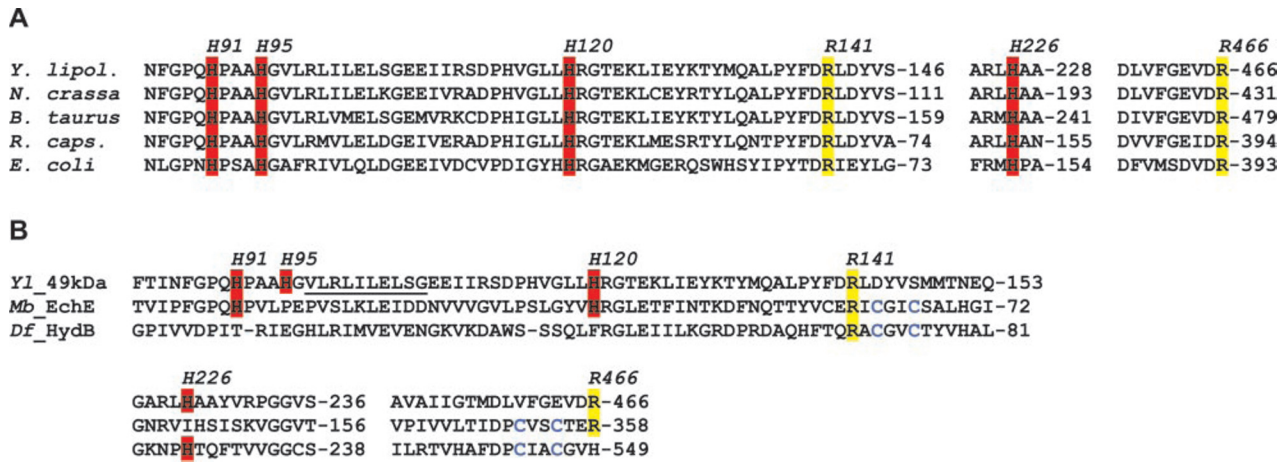

FIG. 1. **Partial alignments of 49-kDa subunit and [NiFe] hydrogenase large subunit sequences.** Alignments were done using the program CLUSTAL W. [Ni] ligating cysteines are in *blue*, histidines are highlighted in *red*, and arginines are in *yellow*. *A*, partial sequences of the 49-kDa subunit from *Y. lipolytica* (*Y. lipol.*), *Neurospora crassa*, *Bos taurus*, *Rhodobacter capsulatus* (*R. caps.*), and *E. coli*. *B*, partial sequences of the 49-kDa subunit of complex I from *Y. lipolytica* (*Yl_49kDa*) aligned with the EchE subunit of the membrane-bound [NiFe] hydrogenase from *Methanosarcina barkeri* (*Mb_EchE*) and the large subunit of the soluble [NiFe] hydrogenase from *Desulfovibrio fructosovorans* (*Df_HydB*). The epitope recognized by a monoclonal antibody (49.2) against the *Y. lipolytica* 49-kDa subunit is *underlined* (15).

leu2–270, *xpr2–322*) (4) with GB12 (*30Htg2*, *Mat*B, *ndh2i*, *his-1*, *ura3–302*, *leu2–270*, *xpr2–322*), followed by sporulation of the resulting diploid and selection of a haploid strain carrying the appropriate markers. To exclude the possibility of aneuploidy the absence of the wild type 49-kDa gene was checked by Southern blotting.

Site-directed Mutagenesis—Point mutations were generated by the QuikChange™ method (Stratagene). The PCR template was a 2870-bp *NUCM* genomic PCR product (4) subcloned into the NheI site of pINA240, which carries the *LEU2* marker or a 3150-bp EcoRI/BamHI fragment (from which an internal BamHI site had been removed by site-directed mutagenesis) subcloned into pUB4, which carries the Hyg^R gene.

Purification of Complex I—*Y. lipolytica* strain Δnucm L1 was grown overnight at 27 °C in a 10-liter Biostat E fermenter (Braun, Melsungen, Germany) in complete medium containing 2% glucose, 2% yeast nitrogen base, and 1% Bacto™ peptone. Mitochondrial membranes were prepared according to published protocols (14, 15) with the modification that the second centrifugation was performed at 140,000 × *g*. Complex I was purified from isolated mitochondrial membranes that were solubilized with *n*-dodecyl-β-D-maltoside essentially as described previously (16), but the Ni^{2+}-affinity column was equilibrated and washed with 55 mM imidazole. Protein content was determined according to a modified Lowry protocol (17). Blue native polyacrylamide gel electrophoresis was performed as described by Schägger (18).

Measurement of Catalytic Activity, K_m, and I_{50}—dNADH was used as electron donor for complex I, and the ubiquinone analogue DBQ was used as electron acceptor. Inhibitor-sensitive dNADH:DBQ activity at 60 μM DBQ and 100 μM dNADH was measured using a Shimadzu MultiSpec-1501 or a Molecular Devices SPECTRAmax PLUS^{384} spectrophotometer by following dNADH oxidation at 340–400 nm (ϵ = 6.22 $mM^{-1}cm^{-1}$) at 30 °C in 50 mM NaCl, 2 mM KCN, 20 mM Na^+/MOPS, pH 7.2. The reaction was started by addition of mitochondrial membranes at 30–50 μg of protein/ml. Michaelis-Menten and I_{50} parameters were determined using microtiter plates in a Molecular Devices SPECTRAmax PLUS^{384} spectrophotometer. dNADH oxidase activity of membranes was measured essentially in the same way, but omitting KCN and DBQ from the assay. The obtained data were fitted using "Enzfitter" (version 2.0.16.0, Biosoft 1999, Cambridge, UK). Specific NADH:HAR oxidoreductase activity was taken as a measure for complex I content and determined as described above in 250 mM sucrose, 2 mM EDTA, 2 mM NaN_3, 20 mM Na^+/HEPES, pH 8.0.

EPR Spectroscopy—Low temperature EPR spectra were obtained on a Bruker ESP 300E spectrometer equipped with a liquid helium continuous flow cryostat, ESR 900 from Oxford Instruments. Samples were reduced with NADH (1–5 mM final concentration), quickly frozen in cold isopentane/methylcyclohexane (5:1), and stored in liquid nitrogen. Generally, protein concentration was 3–10 mg/ml when isolated complex was measured, except for parental and His-226 mutant complex I samples, which were highly concentrated having ~100 mg/ml. When mitochondrial membranes were used, protein concentrations were 20–40 mg/ml. If not indicated otherwise, EPR spectra were recorded at a temperature of 12 K and a microwave frequency of 9.48 GHz. 2-mW microwave power and 0.8-mT modulation amplitude were used for membrane samples, 1 mW and 0.64 mT for isolated complex I, respectively.

RESULTS

Mutations of Histidine 226 Affect the Properties of Iron-Sulfur Cluster N2—His-226 is invariant in all known 49-kDa subunit sequences of complex I (Fig. 1). It corresponds to a highly conserved histidine in water-soluble [NiFe] hydrogenases that forms a hydrogen bond to the proximal iron-sulfur cluster of the small subunit (8). His-226 was mutagenized into alanine and the potential iron-sulfur cluster ligands glutamine, cysteine, and methionine. As judged by blue native-PAGE (data not shown) and NADH:HAR activity (Table I), complex I was fully assembled to normal expression levels in all His-226 mutants.

Only mutation H226A had a pronounced effect on specific, inhibitor-sensitive ubiquinone reductase activity reducing it by 80%. Mutants H226Q and H226C had retained around 50% activity, and membranes from mutant H226M were only slightly less active than those from the parental strain. Hardly any changes were observed in the Michaelis-Menten constant K_m. A slight hypersensitivity of mutant H226 M and a minor resistance of mutant H226A toward the complex I inhibitors DQA and rotenone was observed. For mutants H226C and H226Q, the I_{50} values for DQA and rotenone were unchanged (Table I). No increase of inhibitor-insensitive dNADH:DBQ oxidoreductase or dNADH oxidase activities was observed in membranes from the mutant strains (data not shown).

In EPR spectra recorded from both mitochondrial membranes and purified complex I, marked effects on iron-sulfur cluster N2, but not on the other EPR-detectable iron-sulfur clusters, resulted from all four mutations (Fig. 2). The quality of the spectra obtained with purified complex I was much higher because of markedly increased protein concentrations and the exclusion of interference from other paramagnetic components of the mitochondrial respiratory chain. However, the analysis of EPR spectra of mitochondrial membranes was critical to decide whether iron-sulfur clusters were lost during the purification procedure and allowed a direct comparison with the functional data summarized in Table I. Again, mutation H226A had the most drastic effect resulting in complete loss of characteristic iron-sulfur cluster N2 signals that were not even observed upon reduction of the sample with NADH/dithionite

TABLE I
Characterization of 49-kDa mutants

Strain	Complex I content[a]	Complex I activity[b]	K_m of DBQ	I_{50}		Degree of conservation
				DQA	Rotenone	
		%	μM		nM	
Parental	1.0	100	11	13	600	
H226A[c]	1.0	20		18	770	Invariant in complex I; highly conserved in water-soluble [NiFe] hydrogenases
H226Q	1.1	56	9	13	600	
H226C	1.2	43	5	13	600	
H226M	1.2	80	9	9	300	
R141A[c]	1.3	17	10	21	570	Invariant in complex I and [NiFe] hydrogenases
R141K	1.4	45	13	55	1500	
R141M	1.1	40	11	11	500	
H91A	1.2	<5				Invariant in complex I
H91M	0.8	<5				
H91R	0.8	<5				
H95A	1.3	<5				Invariant in complex I
H95M	1.2	<5				
H95R	1.0	<5				
R466A	0.5	75	11	35	750	Invariant in complex I
R466M	0.7	9				
R466H	1.0	85	25	36	900	
R466E	0.5	53	9	20	700	

[a] Complex I content was determined in at least two batches of mitochondrial membranes, and the mean value is expressed as relative specific NADH:HAR oxidoreductase activity that is not affected by the mutations (parental plasmid-complemented *nucm*::*URA3* deletion strain = 1.0).
[b] Complex I activity was determined in at least two batches of mitochondrial membranes, and the mean value is given as inhibitor-sensitive dNADH:DBQ oxidoreductase activity relative to plasmid-complemented strain and normalized for complex I content (100% = 0.3 μmol $min^{-1}mg^{-1}$).
[c] Data from Kashani-Poor *et al.* (4); included for comparison and completeness.

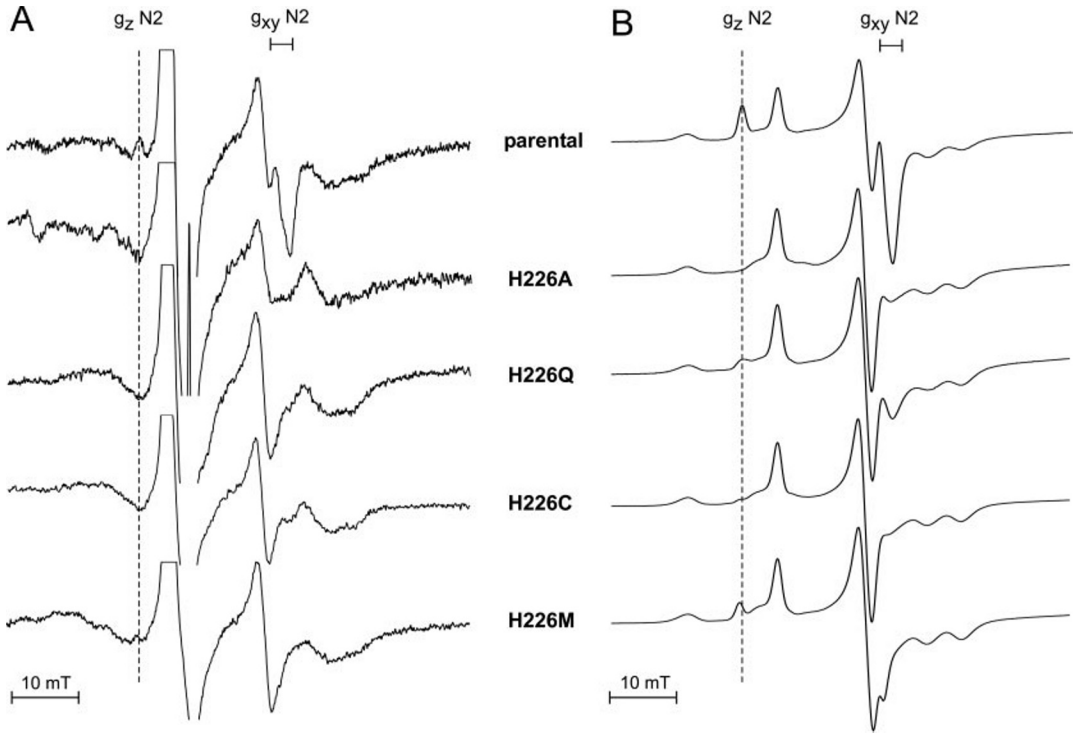

FIG. 2. **EPR spectra from His-226 mutants.** *A*, EPR spectra of mitochondrial membranes from His-226 mutants. Samples were reduced with NADH. The *dashed line* represents the field position of the g_z signal of cluster N2 in the parental sample. *B*, EPR spectra of purified complex I from His-226 mutants reduced with NADH. The spectra show contributions from clusters N1, N2, N3, and N4 (26). The *dashed line* indicates the position of the g_z signal of cluster N2 in the parental strain. The N2 g_z and the g_{xy} field positions in H226M are shifted to lower field values, and the signal has a reduced intensity. H226Q, H226C, and H226A show no shift but a very significant reduction of the N2 signal, which is comparable to the reduction of dNADH:DBQ activity.

($E_h \cong -450$ mV; data not shown). To exclude the possibility that the signal had disappeared due to a dramatic change in the spectroscopic properties of cluster N2, we scanned at different EPR settings (temperature, microwave power, and field ranges) but could not find any new paramagnetic species in mutant membranes or isolated enzyme complex (data not

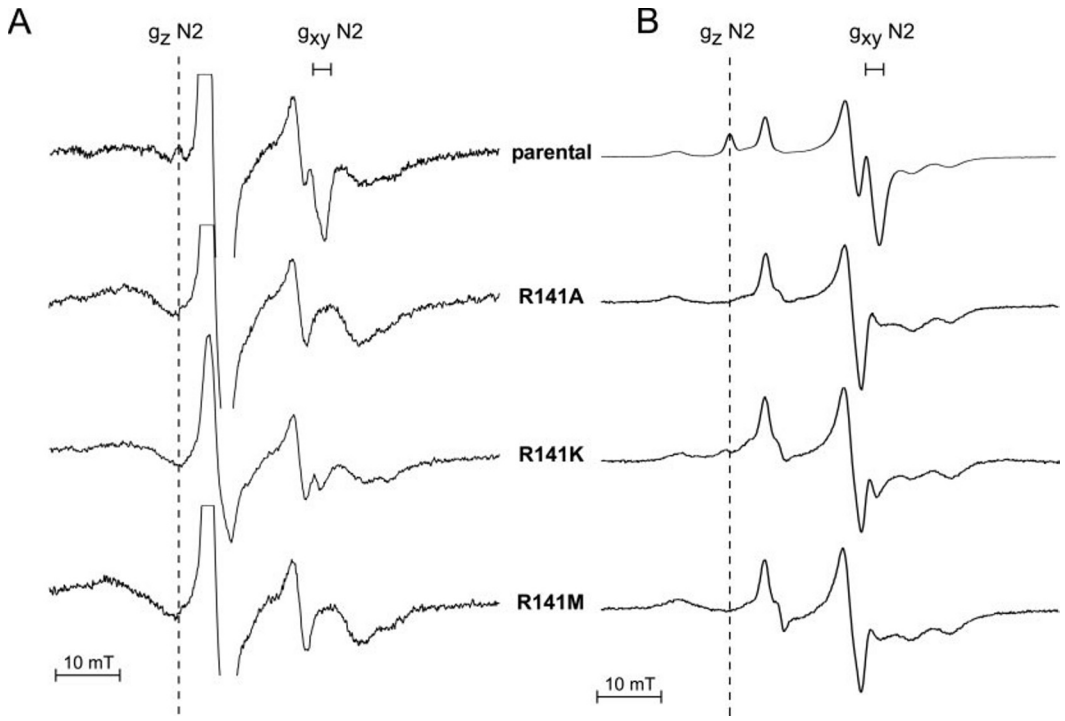

FIG. 3. **EPR spectra from Arg-141 mutants.** *A*, EPR spectra of mitochondrial membranes from Arg-141 mutants. Samples were reduced with NADH. The *dashed line* represents the field position of the g_z signal of cluster N2 in the parental sample. *B*, EPR spectra of purified complex I from Arg-141 mutants reduced with NADH. The spectra show contributions from clusters N1, N2, N3, and N4 (26). The *dashed line* indicates the field position of the g_z signal of cluster N2 in the parental strain. Only in the R141K mutant a cluster N2 g_z signal is observable and is slightly shifted to lower field values.

shown). If the tetranuclear iron-sulfur cluster had been turned into a Fe_3S_4 cluster, it would have become paramagnetic in the oxidized state, resulting in a characteristic EPR spectrum, which was not observed (data not shown).

Similar results were obtained for mutants H226C and H226Q, but residual signals of cluster N2 corresponding to less than 10% of wild type level were observed in EPR spectra of purified complex I within the g_z and g_{xy} regions and of mitochondrial membranes within the g_{xy} region. In membrane preparations from mutant H226M, the g_z signal of cluster N2 was reduced by about two-thirds compared with enzyme from the parental strain. At this level the signal was still hardly detectable in mitochondrial membranes, but as for all His-226 mutations loss of cluster N2 upon purification of complex I could be ruled out. Only in membranes from H226M, a clear g_z signal of cluster N2 could be detected; the g_{xy} signal region was shifted to lower field, now strongly overlapping with the g_{xy} signal of cluster N1. Spectra of purified H226M complex I allowed a more detailed analysis of changes in the N2 EPR signals. The intensity was reduced by about one-third, and all components of the *g*-tensor, obtained by simulation (data not shown), were shifted to lower field values (N2 parental: g_z = 2.051, g_y = 1.926, and g_x = 1.918; N2 H226M: g_z = 2.054, g_y = 1.931, and g_x = 1.923).

Mutations of Arginine 141 Have Moderate Effects on Activity but Drastically Reduce Iron-Sulfur Cluster N2 EPR Signals—Arg-141 is invariant in all known 49-kDa subunits of complex I and large subunits of [NiFe] hydrogenases (Fig. 1). In the hydrogenase structure it is found in close vicinity to the proximal iron-sulfur cluster (8). We have changed this residue to alanine, lysine, and methionine. In all Arg-141 mutants complex I was assembled (data not shown), and complex I content in mitochondrial membranes tended to be even slightly higher than in the parental strain (see Table I).

In a pattern rather similar to the His-226 mutations, mitochondrial membranes from mutant R141A exhibited an inhibitor-sensitive dNADH:DBQ activity that was some 80% reduced, while the two more conservative exchanges R141K and R141M reduced activity only by about 50%. For different batches of mitochondrial membranes from mutant R141K ubiquinone oxidoreductase activity varied quite substantially between 30 and 70% of wild type activity; the value given in Table I is the average of the values from three membrane preparations. The K_m value for DBQ was not changed in any of the three mutants, but mutation R141K resulted in a 4–5-fold higher I_{50} for DQA and a 2–3-fold higher I_{50} for rotenone. Of the two other mutations only R141A seemed to have a subtle effect on DQA sensitivity. Again, no increase of inhibitor-insensitive dNADH:DBQ oxidoreductase or dNADH oxidase activities was observed in membranes from the mutant strains (data not shown).

In stark contrast to these rather normal functional properties, EPR spectroscopy revealed drastic effects specifically on iron-sulfur cluster N2 (Fig. 3); in membranes and purified complex I from mutants R141M and R141A, cluster N2 signals were undetectable. Again, this was not changed following reduction of membrane samples at a lower potential of about −450 mV with NADH/dithionite (not shown). Scanning at different EPR settings or spectra of oxidized samples gave no indications for any newly formed paramagnetic species (data not shown). A small amount of cluster N2 in the order of 5% compared with wild type level was detectable in complex I from mutant R141K; the very weak g_z signal seemed to be shifted toward lower field values.

To further address the question of whether cluster N2 was in fact missing in the mutant membranes or whether the cluster had become just undetectable under standard EPR conditions, we considered the possibility that the mutations had turned the spin of the ground state of cluster N2 to S = 3/2. EPR signals from Fe_4S_4 clusters with S = 3/2 ground states should appear in the g = 4.0–5.5 region but are notoriously difficult to observe, particularly in the event of significant cluster hetero-

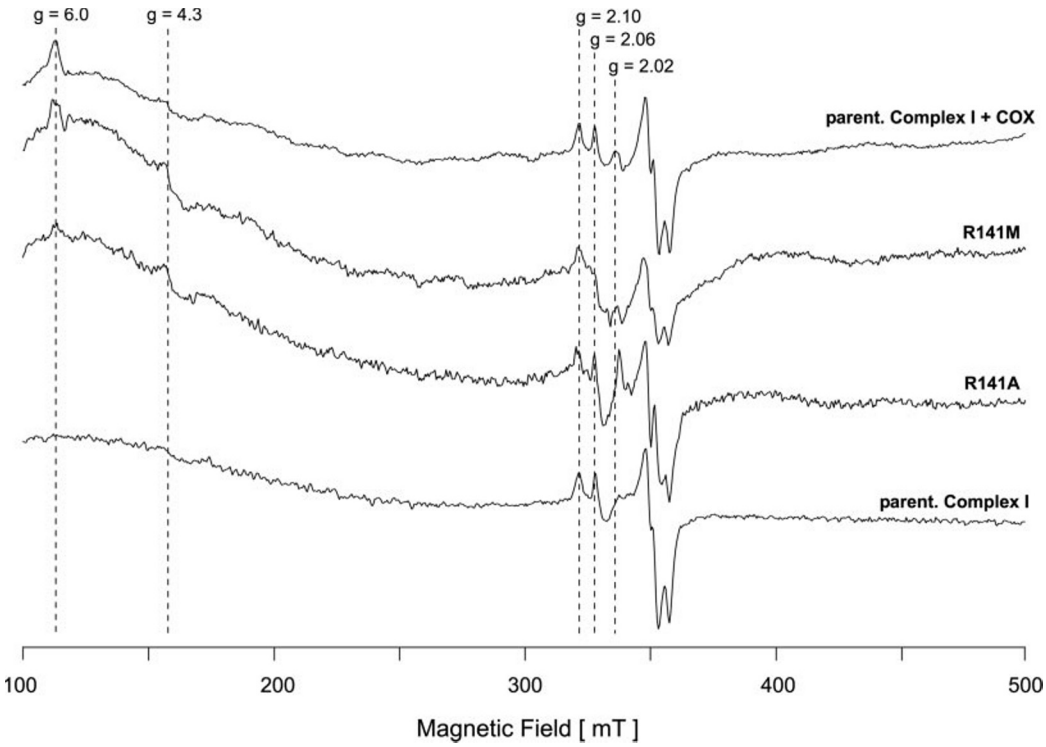

FIG. 4. **Wide range EPR spectra of isolated complex I from parental and mutant enzyme preparations.** To detect possible EPR signals originating from $S = 3/2$ spin states two parental enzyme preparations, one highly pure (*bottom*) and another containing a small amount of cytochrome oxidase (*COX*) as a contaminant (*top*) were compared with mutant preparations R141A and R141M (same samples as in Fig. 3*B*). EPR signals from a $S = 3/2$ state, which should appear in the low field region between $g = 4$ and $g = 5.5$, could not be identified. The signals at $g = 6$ in the mutant samples were attributed to the high spin heme of cytochrome oxidase. At $g = 4.3$ signals from adventitious high spin Fe(III) were detectable. In the region around $g = 2$ the g_z signals of cluster N4 ($g_z = 2.10$), N5 ($g_z = 2.06$), and N1 ($g_z = 2.02$) could be identified. In this field range the EPR signals from cluster N2 are power-saturated completely. All samples had protein concentrations between 5 and 10 mg/ml and were reduced by NADH. EPR conditions were microwave frequency of 9.47 GHz, modulation amplitude of 1 mT, microwave power of 63 mW, and temperature of 4.3 K.

geneity (19, 20). We recorded EPR spectra from parental and mutant isolated complex I samples over a wide field range at low temperature (4.3 K) and high microwave power (63 mW). Fig. 4 shows spectra of complex I from wild type and mutants R141A and R141M for which the discrepancy between catalytic activity and missing N2 EPR signals was most obvious. Under the EPR conditions used, all signals in the 300–400-mT region (from $S = ½$ spin states of clusters N1, N4, and N5) were highly power-saturated, and contributions from clusters N2 and N3 were completely abolished. Apart from more or less pronounced signals at $g = 6$ and $g = 4.3$, which could be assigned to contaminations by cytochrome oxidase and adventitious Fe(III), respectively, there were no additional EPR signals detectable in the mutant complex I samples. However, EPR detection of $S = 3/2$ states is typically performed at high cluster concentrations (~1 mM), a concentration range not accessible for complex I samples. Consequently, the existence of a $S = 3/2$ spin state could not be ruled out completely, due to low complex I concentrations especially in the mutant samples (5–10 μM) and resulting base-line problems in the relevant field region.

Mutations of Histidine 91 and Histidine 95 Result in Complete Loss of Catalytic Activity—Residues His-91 and His-95 are strictly conserved in all complex I 49-kDa subunit sequences but not in [NiFe] hydrogenases (see Fig. 1). Conservation of the structural fold between homologous subunits predicts both residues to be close enough to iron-sulfur cluster N2 to be candidate ligands. His-91 and His-95 were changed into alanine, methionine, and arginine. All His-91 and His-95 mutants contained normal or, in the case of H91M and H91R, only slightly reduced amounts of complex I (see Table I) that was assembled normally (data not shown). In mitochondrial membranes from all six mutant strains inhibitor-sensitive dNADH:DBQ activity was below the detection level of 5%. However, EPR spectra of all iron-sulfur clusters, including cluster N2, were indistinguishable from those of the parental strain (data not shown). This was also true for complex I from mutant H95A that was purified as a representative of this group of mutations.

Mutations of Arginine 466 Change Functional Properties of Complex I—The C-terminal arginine 466 is also strictly conserved in complex I. In [NiFe] hydrogenases it corresponds to a strictly conserved histidine that is ligand to a Mg^{2+} site and resides about 9 Å from the [NiFe] site and 14 Å from the proximal iron-sulfur cluster. Arg-466 was changed into alanine, methionine, histidine, and glutamate. Assembled complex I was found in membranes from all Arg-466 mutants (data not shown), but with the exception of mutant R466H, content was significantly reduced by 30–50%. As a strictly aerobic organism, *Y. lipolytica* does not regulate expression levels for complex I subunits. Hence diminished content usually indicates structural destabilization of the complex. In fact, reduced stability made it difficult to isolate sufficient amounts of protein for EPR spectra of purified complex I from these mutants. Still, inhibitor-sensitive, specific ubiquinone reductase activity was strongly reduced only in membranes from R466M, while the other mutants showed around 80% (R466A and R466H) or about 50% (R466E) of wild type activity (see Table I).

Steady-state kinetics revealed a 2–3-fold increase in the K_m for DBQ for mutant R466H, while this parameter was unaltered in mutants R466A and R466E. These three mutations also exhibited a small but significant resistance toward DQA and rotenone.

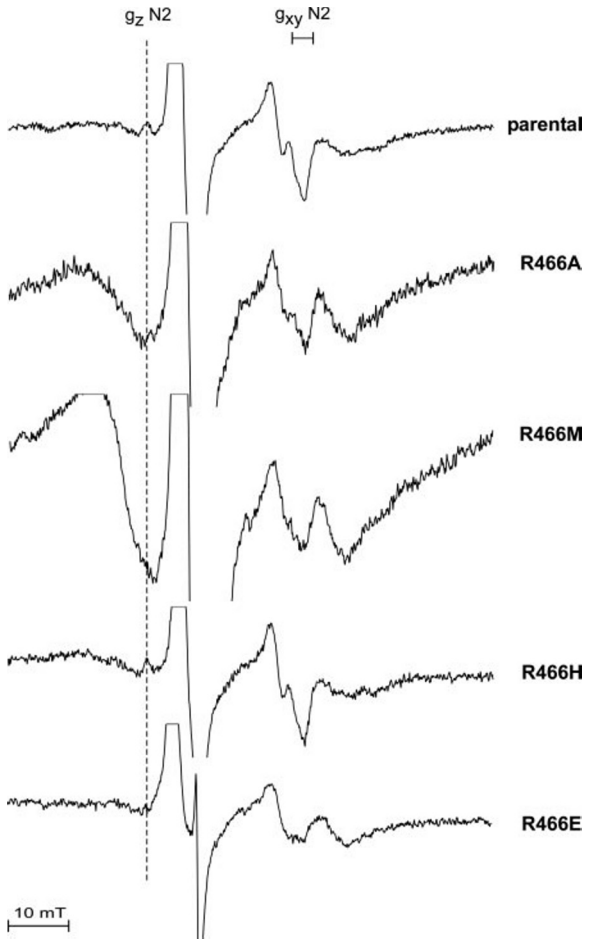

FIG. 5. **EPR spectra of mitochondrial membranes from Arg-466 mutants.** Samples were reduced with NADH. The *dashed line* represents the g_z signal of cluster N2. Only R466H mutant shows a similar spectrum as the parental strain. However, the concentration of complex I was rather low in mutants R466A, R466M, and R466E.

The normally assembled and most active mutant in this set, R466H, also gave rise to EPR spectra of mitochondrial membranes that were indistinguishable from a parental spectrum (Fig. 5). With spectra from mitochondrial membranes only, a detailed analysis of the spectral signature of mutants R466A, R466M, and R466E was not possible. However, it seemed clear that iron-sulfur cluster N2 was drastically reduced in all three mutants, but even in membranes from R466A a trace amount of cluster N2 was clearly detectable in the g_{xy} region.

DISCUSSION

We have explored the function of conserved histidines and arginines of the 49-kDa subunit within the ubiquinone-reducing catalytic core of complex I. One of the specific aims of this study was to test whether these residues may act as the fourth ligand of tetranuclear iron-sulfur cluster N2, completing the set of three cysteine ligands located in the neighboring PSST subunit (21, 22). His-91 and His-95 can be excluded as ligands because even their replacement by alanine had no effect at all on the EPR spectra of cluster N2. Also Arg-466 seems an unlikely candidate because even mutation R466A did not completely abolish the EPR signature of cluster N2. The fact that the cluster was hardly detectable in mitochondrial membranes from three of the four Arg-466 mutants rather seemed to reflect a severe structural destabilization of complex I. Much more specific and remarkably parallel effects on cluster N2 were observed when residues His-226 and Arg-141 were exchanged (see Figs. 2 and 3). In both cases, cluster N2 was not detectable after substitution with a small hydrophobic alanine residue. On the other hand, the more conservative changes R141K and H226M gave rise to reduced but shifted EPR spectra. Other mutations in these positions resulted in dramatic reduction (H226C and H226Q) or virtually complete disappearance (R141M) of cluster N2 EPR signals. Based on these results one could consider both His-226 and Arg-141 as possible fourth ligands of cluster N2. However, the parallel pattern observed for mutagenesis of these two positions rather seemed to suggest that loss of the cluster N2 spectral signature reflected similar structural changes in its surroundings rather than an exchange or removal of its immediate ligand. These structural changes appeared to be local in nature, as, in contrast to mutations of Arg-466, no global destabilization of complex I or loss of residual cluster upon purification was observed. Thus, while we could not identify the fourth ligand of cluster N2, our data demonstrate a specific significance of Arg-141 and His-226 for the local environment of iron-sulfur cluster N2 and provide strong support to the structural model of the ubiquinone-reducing catalytic core of complex I (23).

Mutations of His-91 and His-95 did not provide any information on the ligation or properties of iron-sulfur cluster N2. However, our results still suggested a central functional role for these two residues; independent of the specific amino acid exchange made, all mutations in these two positions resulted in virtually complete loss of catalytic activity without affecting iron-sulfur cluster N2 or dramatically reducing stability of the complex. This behavior is strikingly similar to the results recently obtained for mutagenesis of two conserved aspartates (Asp-99 and Asp-115) in the PSST subunit (5). Based on the structures of homologous water-soluble [NiFe] hydrogenases, histidines 91 and 95 in the 49-kDa subunit and aspartates 99 and 115 in the PSST subunit are predicted to be located on opposing surfaces of the two proteins. Therefore, it is tempting to speculate that they might form specific ion pairs critically involved in the catalytic mechanism of complex I. It should also be noted that the two histidines reside in a loop connecting the first two strands of a predicted β-sheet of the 49-kDa subunit; recently, by electron microscopic single particle analysis of co-complexes of *Y. lipolytica* complex I and monoclonal antibody 49.2 we localized the second putative β-strand of this predicted β-sheet bound by glycines 96 and 106 near the end of the peripheral arm of complex I opposite to its connection to the membrane part (15). We consider the identification of two functionally deficient mutants in this part of complex I as another indication that critical parts of the catalytic machinery of complex I are clearly separated from the membrane domain.

We made a puzzling observation for a number of mutants when we compared spectroscopic properties and catalytic activities; the pronounced effects on the EPR spectra of cluster N2 caused by mutagenesis of His-226, Arg-141, or Arg-466 were in stark contrast to comparably moderate reductions in inhibitor-sensitive ubiquinone reductase activities. In the three alanine mutations hardly any cluster N2 was detectable, but still around 20% (H226A and R141A) or even 75% (R466A) specific activity could be measured. This was most evident in the case of mutation R141M, where cluster N2 was not detectable but inhibitor-sensitive, specific dNADH:DBQ activity was still 40%. We could rule out that these rates were due to an artificial reaction with decylubiquinone that does not occur with endogenous ubiquinone-9; inhibitor-insensitive residual rates were not increased in mutant membranes, no matter whether we measured dNADH oxidase or dNADH:DBQ oxidoreductase activity. The most obvious explanation for this apparent paradox would be that the redox center assumed to be the immediate electron donor for ubiquinone was still present

in the mutant enzymes but could not be detected anymore by standard procedures. In principle, this could have been caused by two types of changes in the properties of iron-sulfur cluster N2. (i) The mutations could have altered the redox potential of the cluster to very negative values, preventing reduction by NADH or NADH/dithionite. However, this seems highly unlikely; the absence of even residual reduction in some mutants would correspond to midpoint potentials of below −450 mV, reflecting a shift of at least −300 mV. (ii) The mutations could have profoundly changed the magnetic properties of the cluster making it undetectable by the standard EPR conditions used; the option that the tetranuclear iron-sulfur cluster was turned into a Fe_3S_4 cluster by the mutations was ruled out by analyzing oxidized samples. Reduced samples were scanned at many different EPR settings (temperature, microwave power, and field ranges), but we could not find indications for a new paramagnetic species in the mutant membranes or isolated enzyme complexes. Even a wide range scan at very low temperature (4.3 K) and high microwave power (63 mW) to explore the possibility that the spin of the ground state of the cluster might have turned into $S = 3/2$ gave no hints at an altered state of the cluster. While in a strict sense, it is impossible to actually prove the absence of an iron-sulfur cluster by EPR spectroscopy, it still seemed rather unlikely to us that a conversion of the cluster N2 ground state into the unusual $S = 3/2$ species had been caused in a similar fashion by several mutations at different positions in the 49-kDa subunit. Therefore, we concluded from our extensive EPR spectroscopic analysis that some mutations of His-226 and Arg-141 probably had resulted in the loss of most or all of iron-sulfur cluster N2. It should be noted at this point that in previous studies exploring the ligation of iron-sulfur cluster N2 (10–12) only standard EPR conditions were applied, and the possible explanations for the disappearance of the typical EPR signature outlined above were not even considered. Therefore, the data and conclusions drawn from these studies have to be reconsidered critically in the light of the discussion presented here.

If in some of the mutants that still showed rather high specific catalytic activities the disappearance of the EPR spectrum of cluster N2 indeed reflected loss of this redox center, the question arises how this apparent paradox could be resolved. In fact, electron transfer theory offers a straightforward though at this point speculative explanation; in electron wires consisting of a series of iron-sulfur clusters or other components, distances between redox centers are typically around 5 Å (8, 9). This should be a good approximation for the iron-sulfur clusters of complex I as well. Estimating electron transfer rates using the "Moser-Dutton ruler" (24), this distance corresponds to a rate of at least 10^8–10^9 s^{-1} if no driving force is assumed. In a simple scenario, the electron would have to travel around 10 Å if one redox center in a chain of iron-sulfur clusters was removed. The estimated electron transfer rate would then drop by about two orders of magnitude but still would be in the range of 10^6–10^7 s^{-1}. Comparison of these estimates with the steady-state turnover number of about 10^2 s^{-1} illustrates that removal of iron-sulfur cluster N2 does not necessarily limit steady-state turnover because electron transfer is still predicted to be much faster. A similar situation, although involving entirely different redox centers, has been analyzed recently by time-resolved absorption spectroscopy on the picosecond time scale in mutants of *Escherichia coli* DNA photolyase (25). Unfortunately, no methods are available so far to study electron transfer within complex I even in the submillisecond time range.

If, as suggested by our results, complex I can catalyze ubiquinone reduction at essentially normal rates even in the absence of cluster N2, this questions some of the central mechanistic functions that have been discussed for iron-sulfur cluster N2. The key issue that is now under investigation in our laboratory is whether the mutations discussed in this work interfere with the proton pump of complex I.

Acknowledgments—We thank Andrea Böttcher, Franz-Josef Streb, Gudrun Beyer, and Jolanta Maria Brzoska for excellent technical assistance and Stefan Dröse, Hermann Schägger, and Volker Zickermann for helpful discussions. We are grateful to an anonymous reviewer who pointed us to the fact that Fe_4S_4 clusters may exist in a $S = 3/2$ ground state under certain conditions.

REFERENCES

1. Brandt, U., Kerscher, S., Dröse, S., Zwicker, K., and Zickermann, V. (2003) *FEBS Lett.* **545,** 9–17
2. Magnitsky, S., Toulokhonova, L., Yano, T., Sled, V. D., Hagerhall, C., Grivennikova, V. G., Burbaev, D. S., Vinogradov, A. D., and Ohnishi, T. (2002) *J. Bioenerg. Biomembr.* **34,** 193–208
3. Kerscher, S., Dröse, S., Zwicker, K., Zickermann, V., and Brandt, U. (2002) *Biochim. Biophys. Acta* **1555,** 83–91
4. Kashani-Poor, N., Zwicker, K., Kerscher, S., and Brandt, U. (2001) *J. Biol. Chem.* **276,** 24082–24087
5. Garofano, A., Zwicker, K., Kerscher, S., Okun, P., and Brandt, U. (2003) *J. Biol. Chem.* **278,** 42435–42440
6. Böhm, R., Sauter, M., and Böck, A. (1990) *Mol. Microbiol.* **4,** 231–243
7. Albracht, S. P. J. (1994) *Biochim. Biophys. Acta* **1188,** 167–204
8. Volbeda, A., Charon, M. H., Piras, C., Hatchikian, E. C., Frey, M., and Fontecilla-Camps, J. C. (1995) *Nature* **373,** 580–587
9. Montet, Y., Amara, P., Volbeda, A., Vernede, X., Hatchikian, E. C., Field, M. J., Frey, M., and Fontecilla-Camps, J. C. (1997) *Nat. Struct. Biol.* **4,** 523–526
10. Friedrich, T., Brors, B., Hellwig, P., Kintscher, L., Rasmussen, T., Scheide, D., Schulte, U., Mäntele, W., and Weiss, H. (2000) *Biochim. Biophys. Acta* **1459,** 305–309
11. Duarte, M., Populo, H., Videira, A., Friedrich, T., and Schulte, U. (2002) *Biochem. J.* **364,** 833–839
12. Flemming, D., Schlitt, A., Spehr, V., Bischof, T., and Friedrich, T. (2003) *J. Biol. Chem.* **278,** 47602–47609
13. Ohnishi, T. (1998) *Biochim. Biophys. Acta* **1364,** 186–206
14. Kerscher, S., Okun, J. G., and Brandt, U. (1999) *J. Cell Sci.* **112,** 2347–2354
15. Zickermann, V., Bostina, M., Hunte, C., Ruiz, T., Radermacher, M., and Brandt, U. (2003) *J. Biol. Chem.* **278,** 29072–29078
16. Kashani-Poor, N., Kerscher, S., Zickermann, V., and Brandt, U. (2001) *Biochim. Biophys. Acta* **1504,** 363–370
17. Lowry, O. H., Rosebrough, N. R., Farr, A. L., and Randall, R. J. (1951) *J. Biol. Chem.* **193,** 265–275
18. Schägger, H. (2003) in *Membrane Protein Purification and Crystallization: A Practical Guide* (Hunte, C., von Jagow, G., and Schägger, H., eds) pp. 105–130, Academic Press, San Diego, CA
19. Conover, R. C., Kowal, A. T., Fu, W. G., Park, J. B., Aono, S., Adams, M. W., and Johnson, M. K. (1990) *J. Biol. Chem.* **265,** 8533–8541
20. Duderstadt, R. E., Brereton, P. S., Adams, M. W., and Johnson, M. K. (1999) *FEBS Lett.* **454,** 21–26
21. Friedrich, T. (1998) *Biochim. Biophys. Acta* **1364,** 134–146
22. Videira, A. (1998) *Biochim. Biophys. Acta* **1364,** 89–100
23. Kerscher, S., Kashani-Poor, N., Zwicker, K., Zickermann, V., and Brandt, U. (2001) *J. Bioenerg. Biomembr.* **33,** 187–196
24. Page, C. C., Moser, C. C., Chen, X., and Dutton, P. L. (1999) *Nature* **402,** 47–52
25. Byrdin, M., Eker, A. P., Vos, M. H., and Brettel, K. (2003) *Proc. Natl. Acad. Sci. U. S. A.* **100,** 8678–8681
26. Djafarzadeh, R., Kerscher, S., Zwicker, K., Radermacher, M., Lindahl, M., Schägger, H., and Brandt, U. (2000) *Biochim. Biophys. Acta* **1459,** 230–238